Int. J. Electrochem. Sci., 14 **(2019)** 6018 – 6031, doi: 10.20964/2019.07.32

International Journal of
ELECTROCHEMICAL
SCIENCE
www.electrochemsci.org

Effect of bis-(3-triethoxysilylpropyl)-tetrasulfide on Super-Hydrophobicity and Corrosion Resistance of Self-Assembled Monolayers on 6061 Aluminum Alloys

Y.Q. Wen, D. Kong, W. Shang[*], *M.M. Ma, J.Q. Jiang, J.P. Li, N. Peng*[*]

Guilin University of Technology, No. 12, Jiangan Road, Guilin City, Guangxi, China.
[*]E-mail: 2001018@glut.edu.cn;

Received: 1 February 2019 / *Accepted:* 5 May 2019 / *Published:* 10 June 2019

The super-hydrophobic self-assembled monolayers (SAMs) were prepared by self-assembled and etching method on 6061 aluminum alloys. Its wettability, morphology, and chemical composition of SAMs were investigated by contact angle (CA), field-emission scanning electron microscopy (FE-SEM), Fourier transform infrared spectroscopy (FTIR), X-ray photoelectron spectroscopy (XPS), and energy dispersive spectroscopy (EDS). The corrosion resistances of SAMs were studied by potentiometric polarization and AC impedance in 3.5 wt.% NaCl solution. The result indicated that self-assembled film had super-hydrophobic properties when bis-(3-triethoxysilylpropyl)-tetrasulfide (BTESPT) volume was 0.10mol/L. Electrochemical properties testing showed that the film had better corrosion resistance, in which the corrosion current density was maintain 1.140 $\times 10^{-7}$ A/cm^2 and AC impedance reached 2.30 $\times 10^5$ Ω•cm^2. Therefore, the film has both superhydrophobic and corrosion resistance characteristics.

Keywords: Aluminum alloy, Super-hydrophobicity, Self-assembled, Corrosion resistance

1. INTRODUCTION

Aluminum alloy is widely used in the field of electronic and aerospace industry because of its light weight, low cost, high electrical conductivity, easy to recycle and so on [1-3]. However, the surface of the aluminum alloy was susceptible to corrosion because the surface oxide film was often destroyed in the corrosive environment. At present, the common method used to improve the corrosion resistance of aluminum alloy surface treatment methods are: Anodizing[4,5], chromate passivation, phosphate conversion film[6,7] , rare earth conversion molecular treatment [8-10], Chemical etching [11,12], etc. However, these methods are not friendly to the environment. It is of great significance to research and develop aluminum alloys, which are non-toxic, environmentally-friendly and corrosion-resistant [13-15].

With the improvement of environmental protection practical application, self-assembled monolayers (SAMs) in the aluminum alloy to improve the corrosion resistance, to pollution-free, low cost and other advantages gradually highlights its own advantages. Self-assembled monolayers have been paid more and more attention and have been developed rapidly. Molecular self-assembly technology had been widely used in basic research and engineering fields. At present, the rapid development of molecular self-assembly technology to effectively overcome the shortcomings of the traditional membrane technology, this technology was not only simple, fast and film stability and order are better. Self-assembled molecular had opened up a great prospect for the protection of metal materials.

It is well known that sulfur-containing silane coupling agent (SCA) is one of the essential additives in the vulcanization process of natural rubber and synthetic rubber products [16,17]. SCA can significantly improve the interface bonding properties of inorganic phase-organic phase. Through, the self-assembly of SCA molecules on the surface of aluminum alloy, it is expected that the metal/organic coating is formed with strong hydrophobic properties. The free size of the interface phase, which significantly improved the organic coating system corrosion protection performance, has played an increasingly important in the field of metal surface pretreatment of new technologies [18-20]. On the other hand, the hydrophobicity of metal surface is also one of the hot spots. The increase of hydrophobicity is helpful to improve the corrosion resistance of metal in electrolyte solution. The super-hydrophobicity of the metal can prevent the electrolyte solution from entering the interface, minimize the contact area with the corrosive ions and resist to corrosion. Recently, although there are many techniques to prepare super-hydrophobic surfaces, few products can be widely used in practice, mainly due to their poor mechanical properties and poor chemical stability[21,22].It is noteworthy that many methods of creating super-hydrophobic surface are susceptible to temperature and physical friction, or outside the harsh conditions such as strong acid and alkali damage[23]. In recent years, some literatures have reported that aluminum alloy super-hydrophobic membrane preparation, to effectively prevent corrosion. For instance, Cansen Liu et al [24]. Fabrication of a robust and corrosion resistant super-hydrophobic aluminum alloy surface by general method, conventional preparation of thin film process was relatively complex, in addition to consume a lot of energy. Wail Al Zoubi et al[25].Prepared flowerlike organic−inorganic coating responsible for extraordinary corrosion resistance via self-assembly of an organic compound in AZ31 Mg alloy. The electrochemical resistance was improved significantly due to the synergistic influences of the inorganic coating via plasma electrolysis and organic coating via self-assembly of PPC. In this paper, super-hydrophobic self-assembled monolayers were prepared by chemical etching and self-assembly. The characteristics and composition of the SAMs were studied by SEM, FT-IR, XPS and contact angle meter. The corrosion resistance of SAMs was researched by potentiometric polarization and electrochemical impedance spectroscopy (EIS) in 3.5 wt.% NaCl solution.

2. EXPERIMENTAL

2.1 Materials

The chemical composition was shown in Table 1. The experimental material used 6061 aluminum alloy sample size was 30 mm × 40 mm × 3 mm. bis-(3-triethoxysilylpropyl)-tetrasulfide （BTESPT, AR, Jiangxi Xinyi Agricultural Chemical Co., Ltd.）, acetone, hydrochloric acid, Potassium sulfide, Polyethanol 200 (AR, Guangdong Shantou City West Long Chemical Co., Ltd). The aluminum alloy substrates were polished with 600 #, 800 # and 1200 # by grit sand paper rinsing with distilled water. The aluminum alloy substrates were ultra-sonically cleaned by acetone and deionized water for 10 min. The clean aluminum alloy substrates were treated by 3.75 mol/L HF for 10 min, 4 mol/L HCl for 12 min. Finally, deionized water cleaning, drying with a blast dryer at 70-100 ℃.

Configure different concentrations of solution was prepared: 37.5 mL anhydrous ethanol, 5 mL polyethylene glycol 200, 5 mL potassium sulfide, with acetic acid to adjust the pH of 4.0 solutions, stir in the 35 ℃ magnetic stirrer 1 h, immediately the next step deal with. Several concentrations were 0.06 mol/L, 0.10 mol/L, 0.14 mol/L, and 0.18 mol/L, respectively. The pretreated 6061 aluminum alloy was placed in the BTESPT solution at a temperature of 35 ℃, self-contained 1h after removal, deionized water washed several times to remove the surface of unreacted small molecules and solvents, 100 ℃ for several hours. Subsequently, the sample was tested for performance. The fabrication route was shown in figure 1.

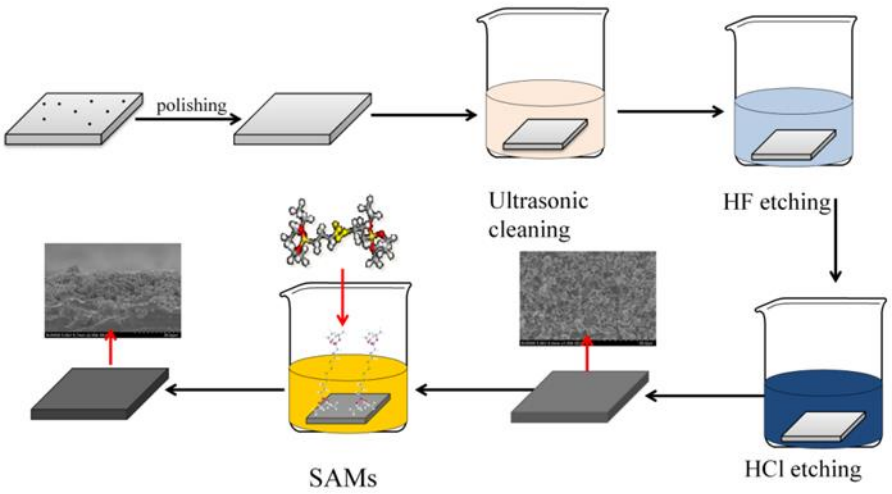

Figure 1. Fabrication route for the SAMs.

Table 1. Chemical composition (wt.%) of 6061 aluminum.

Element	Cu	Mn	Mg	Zn	Cr	Ti	Si	Fe	Al
Weight(%)	0.15~0.4	0.15	0.8~1.2	0.25	0.04~0.35	0.15	0.4~0.8	0.7	balance

2.2 Measure methods

Scanning electron microscopic (SEM) and Energy-dispersive X-ray spectroscopy (EDS) images and spectrums were used to a Hitachi SU5000 emission scanning electron microscope. The SEM acceleration voltage was carried out by 5.0 kV at working distance from 5.00 to10.00 μm. The EDS of the spectrum is the half width of Mn- Ka (5.89). When the input count is about 2500 cps, the half width of Mn -Ka was measured. In the experiment, the test was 120.6eV. The static contact angle tester (XG-CAMA) was used to illustrate the contact angle (WCA) to show super-hydrophobic properties, at room temperature and atmospheric pressure, deionized water having a volume of about 5 μL was dropped onto the aluminum alloy substrate. At least five parallel points are tested on a substrate surface to obtain the mean value of the contact angle. The chemical characteristics of the BTESPT SAMs were characterized by Fourier transform infrared spectroscopy (FT-IR, Spectrum 100 PerkinElmer) and X-ray photoelectron spectroscopy (XPS, ESCALAB 250Xi). The FTIR apparatus is 16, the number of scanning is 20 and the interval data is 1.929cm^{-1}. The XPS spectrometer was used to determine the content and valence of the sample and irradiate with monochromatic Al Kα (1486.6 eV) and infrared spectrum was collected in a reflection mode with a wave number of 4000-500 cm-1. The full spectrum is 100 eV and the step length are 1 eV. The narrow spectrum has a pass energy of 20 eV and a step length of 0.1 eV. The degree of vacuum tested was 10-10 mbar, and all measured sample lines were calibrated using the C1s (BE = 284.8 eV) standard contamination peak. The full spectrum acquisition parameters: total acquisition time is1 mins 8.0 secs, number of scans is 1 Lens mode is standard, analyzer mode is CAE, pass energy is 100.0 eV, energy step size is 1.000 eV and number of energy steps is 1361.

The exposed area of the sample was 1.0×1.0 cm^2. The AC impedance and potentiodynamic polarization curves were carried out in 3.5 wt.% NaCl at room temperature via an electrochemical workstation (CH, Instruments, Model 760E Co., Ltd.). The Electrochemical performance test system was three-electrode system consisting of a working electrode, an auxiliary electrode and a reference electrode, which the self-assembled aluminum alloy sheet was used as the working electrode (WE), the platinum (Pt) sheet was used as the auxiliary electrode (CE) and the saturated calomel electrode (SCE) as the reference electrode. Before the start of the test, the sample was subjected to an open-circuit potential scan in the electrolyte at 25℃ until the open circuit potential was stable. After the open circuit potential is stable, the polarization curve has a potential scan range of ± 300 mV (relative to the open circuit potential) and a scan rate of 1 mV/s. The frequency range of the AC impedance was 10^{-2} Hz to 10^5 Hz, and the applied sinusoidal applied voltage was 10 mV.

3. RESULTS AND DISCUSSION

3.1The Morphologies and composition of the SAMs

Different BTESPT concentrations of SAMs were characterized by SEM, as shown in figure 2. The inset of Figure 2 shows the contact angle of SAMs. The order of a-d was presented the

concentrations of BTESPT 0.06 mol/L, 0.10 mol/L, 0.14 mol/L and 0.18 mol/L in figure 2. It can be seen the surface had different roughness of concave convex structure. Compared with Figure 2b, the surface roughness of the other three concentrations of SAMs were more inhomogeneous. Form the figure 3, With the increase of self-assembly molecular concentrations, the contact angle of water droplets on the surface of SAMs firstly increases and then decreases. When the concentration was 0.10 mol/L, the contact angle reaches 158±2°, which had super-hydrophobic properties. It was found that the solution of 0.10 mol/L of BTESTP was the most advantageous to form superhydrophobic interface structure. It can be inferred that the formation of a uniform roughness film on the surface was more conducive to the formation of superhydrophobic properties. This may be due to the fact that the uniform and rough surface structure is conducive to the sealing of air droplets into discontinuous cavities and the formation of superhydrophobic effect.

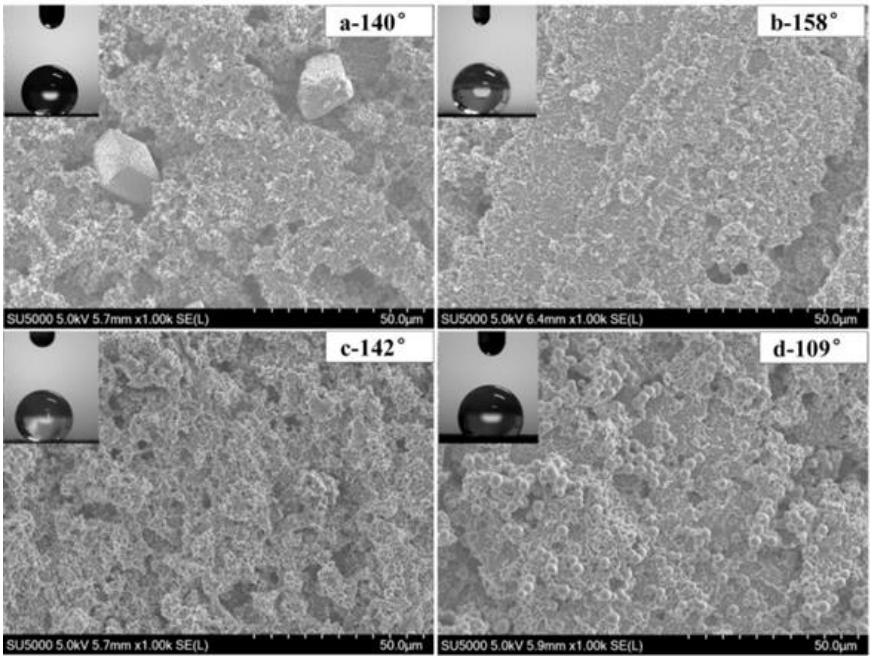

Figure 2. The SEM and contact angle of the film with different self-assembled molecular concentrations (a) 0.06 mol/L;(b) 0.10 mol/L;(c) 0.14 mol/L; (d) 0.18 mol/ L.

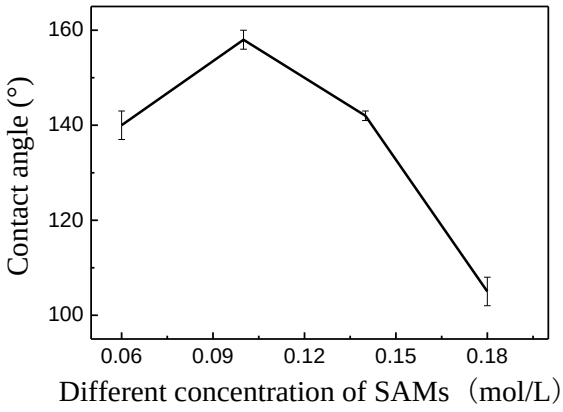

Figure 3. Contact angle of the SAMs with different self-assembled molecular concentrations.

Figure 4 was the cross section of self-assembled films, and Figure 5 was the cross section of the self-assembled films prepared by combining self-assembled and etching techniques. As can be seen from figure 4a, thickness of self-assembled films was small, with a certain degree of roughness, the thickness was about 3 - 4 μm. After the chemical etching, self-assembled film modified surface roughness structure was more obvious. These concavo-convex step-like distribution increases the micro-roughness, the film thickness also increased to about 8-10μm, which was improved the hydrophobicity of the metal surface [26-27].

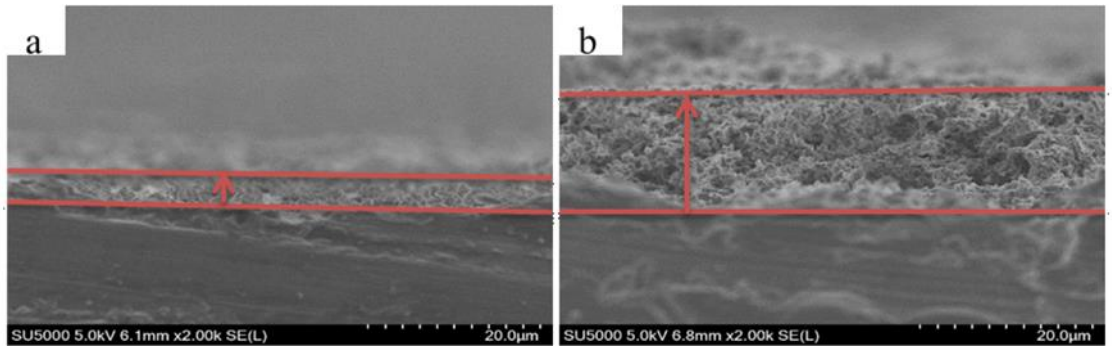

Figure 4. SEM micrographs of cross section (a) the self-assembled films, (b) the self-assembled films prepared by combining self-assembled and etching.

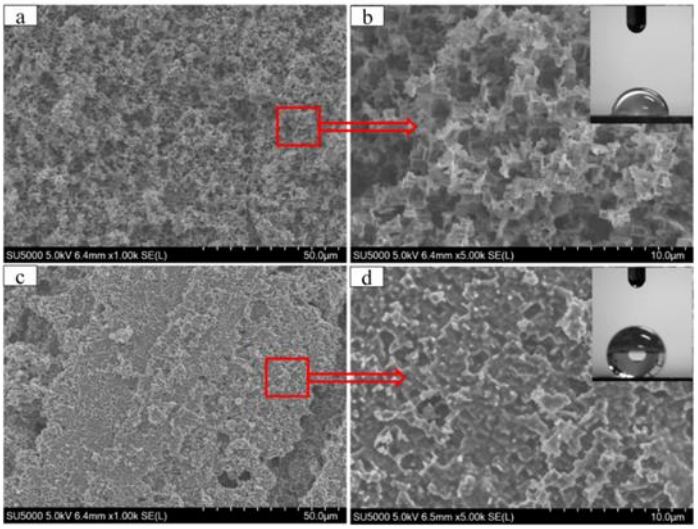

Figure 5. Aluminum alloy matrix etching and etch self-assembled film of SEM image (a-b) chemical etching, (c-d) chemical etching self-assembled film (b and d are magnified, respectively).

The surface SEM diagram of the matrix and super-hydrophobic self-assembled film after chemical etching were shown in Figure 5. The figure 5a was the electron micrograph of the matrix after chemical etching and figure 5c was the surface SEM diagram of the super-hydrophobic film. Graphs Figure 5b and 5d were magnified SEM images of graphs figure 5a and 5c, respectively. It was observed that chemically etched substrate surface has a lot of rugged, pore size of the concave hole, due to the size of the pore size causes, the contact angle of water droplets on the surface was only

45±2.5°. After etching the self-assembled film surface, further optimization of the etching caused by different pore sizes of this structure, making the surface covered with dense, uniform pore size of the films. The contact angle of water droplet reached to 158±2°, which had super-hydrophobic property.

The chemical composition and morphology of self-assembled super-hydrophobic membrane were analyzed by FTIR, XPS and EDS spectroscopy. To demonstrate that the BTESPT was successfully applied to the surface, the chemical composition of the modified sample and unmodified sample were analyzed by EDS. The results were shown in Figure 6. Table 2 was EDS data for the surface composition of samples. By showing the silicon peak and the sulfur peak in the EDS, it was confirmed that the SAMs was contained a BTESPT spectrum compared to the matrix of the aluminum alloy.

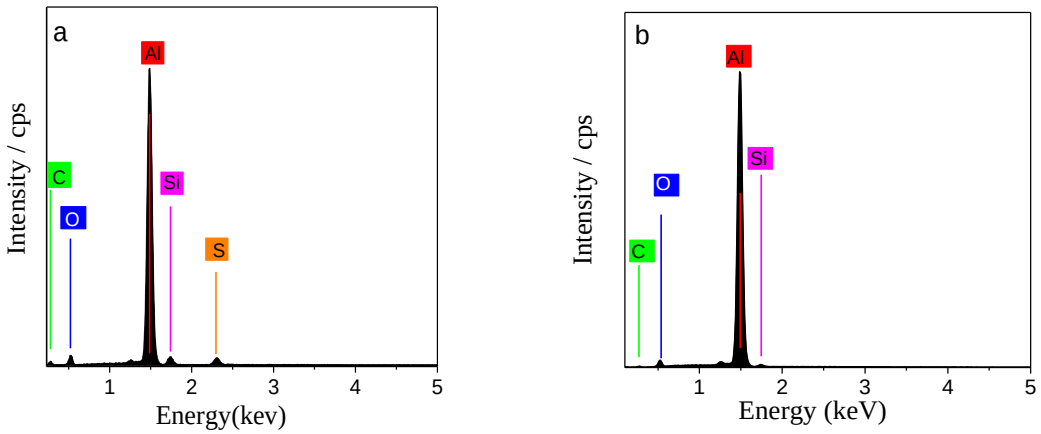

Figure 6. The EDX of SAMs(a); Aluminum alloy(b).

Table 2. EDS data for the surface composition of samples.

Sample	Al	C	O	Si	S
Al alloy matrix	96.96	3.85	1.86	0.47	-
SAMs	76.19	14.45	6.82	1.75	0.78

The FTIR of the Self- assembled films was obtained in Figure 7. The results were obtained that 2927 cm^{-1}, 2887 cm^{-1}, 1442 cm^{-1} were the asymmetric stretching vibration peaks of CH_2[28-30], the symmetrical stretching vibration peaks of CH_3, and the shear vibration peaks of CH_2 in $SiOCH_2CH_3$. 1390 cm^{-1} and 1243 cm^{-1} were the asymmetric stretching vibration peaks of CH_3 and the oscillating vibration peaks of CH_2 in $SiOCH_2CH_3$, respectively [31]. The 1090 cm^{-1} was the vibration peak of SiOC, 954 cm^{-1} was the asymmetric stretching vibration peak of SiO in $SHCH_2CH_3$[32], 790 cm^{-1} was the symmetrical stretching vibration absorption peak of SiC[33]. Moreover, the 3382 cm^{-1} was the stretching vibration peak of the association OH[34]. From these peaks, it was shown that the groups contained in the BTESPT molecule correspond to the self-assembled molecular layer on the aluminum alloy substrate. The formation of self-assembled molecular coatings had played a very critical role in protecting the aluminum alloy substrate.

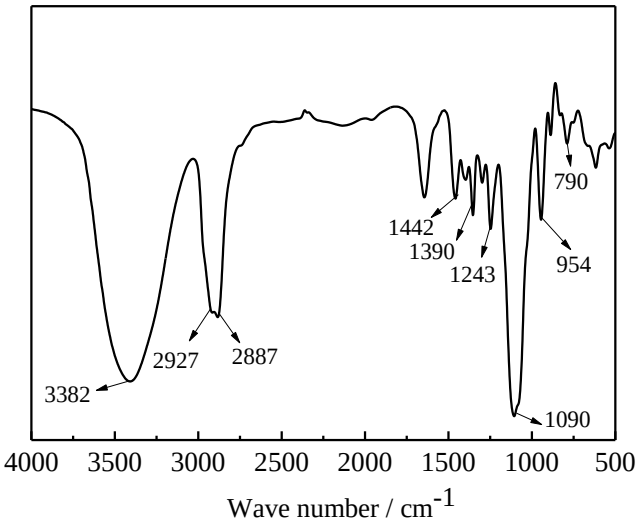

Figure 7. FTIR spectra of the SAMs.

Figure 8 showed the XPS of the SAMs. According to the Figure 8, it can be seen from C, O, Si, S of four main elements, while elements C, O and S were the main constituents of self-assembled molecules. Because the sample surface and interface 1-10 nm can be provided, the Al element cannot be detected. Table 3 was XPS data for the surface composition of samples. Figure 9c was shown the high-resolution peaks of C 1s consisting of strong peaks at 284.80 eV, 286.42 eV, 288.74 eV, corresponding to C -C, C-O, C = O bonds[35]. The O 1s peak composed to one peak having binding energy 532.10 eV corresponds to the bonding of Al -OH, respectively[36]. The respective bands of Si 2p and S peaks were 102.42 eV and 163.73 eV (Figure 9a and 9d)[37]. It was confirmed that the self-assembled monolayers were successfully prepared on the surface of the aluminum alloy.

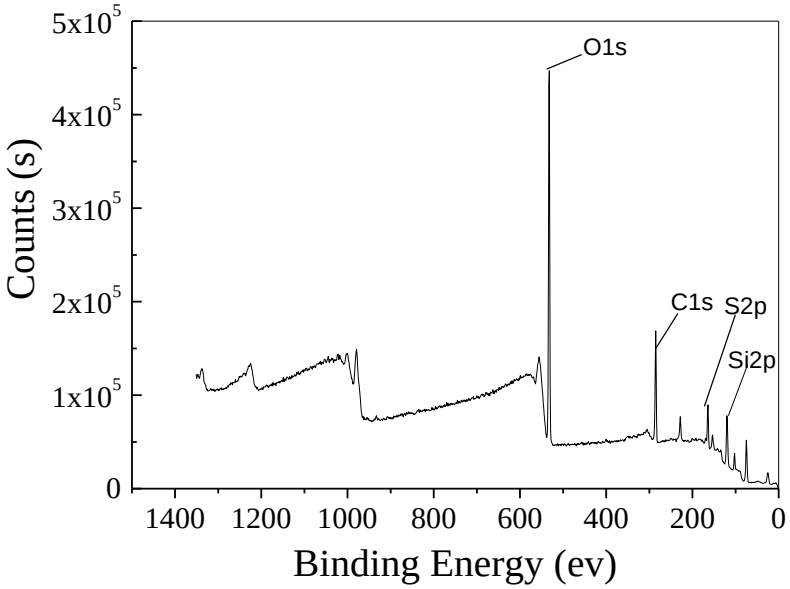

Figure 8. XPS spectra of the SAMs.

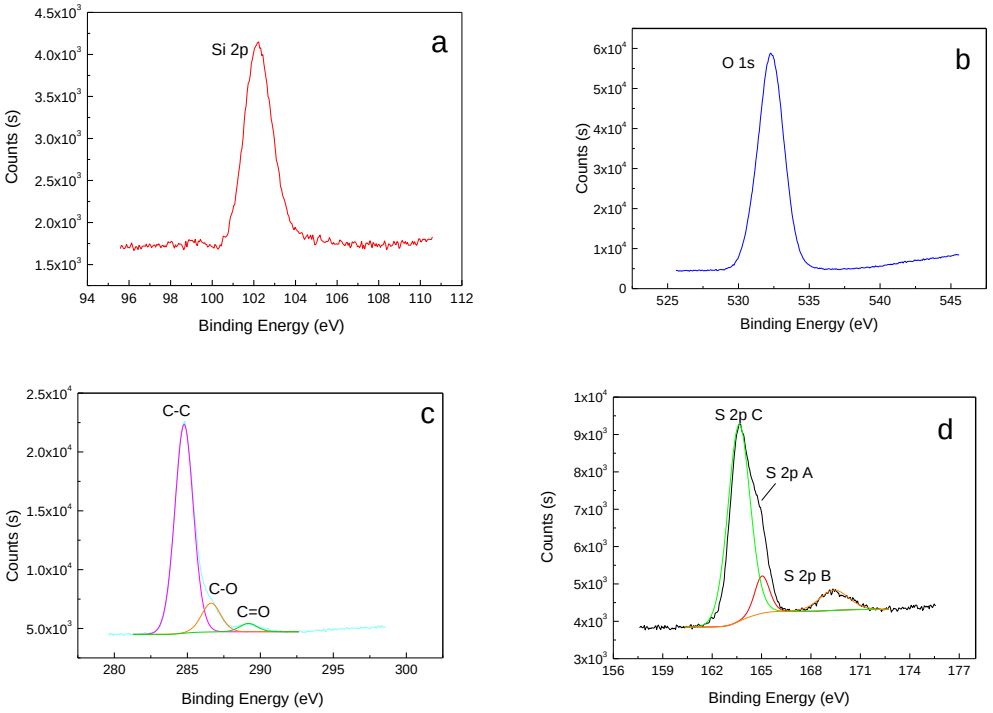

Figure 9. High resolution spectra of the element Si(a); O(b); C(c); S(d).

Table 3. XPS data for the surface composition of samples.

Name	Si 2p	S 2p	C-C	O 1s	C-O	C=O
Atomic %	2.18	6.07	15.61	73.32	2.23	0.59

3.2 Electrochemical performance

AC impedance was performed to estimate the healing effect. The corrosion resistance of the SAMs was measured by the potentiodynamic polarization. The results were shown in Figure 10. The curves of 1, 2, 3 and 4, respectively, indicate that the BTESPT concentrations were 0.06 mol/L, 0.10 mol/L, 0.14 mol/L and 0.18 mol/L. In Figure 10, the corrosion potentials were -0.648 V, -0.675 V, -0.710 V, -0.750 V, respectively. These corrosion currents were 3.8106×10^{-5} A/cm^2, 1.14×10^{-7} A/cm^2, 2.0573×10^{-5} A/cm^2, 2.0165×10^{-5}A/cm^2. On the hand, by comparing the corrosion potential correction of curve 2, it was found that the self-assembled was less susceptible to corrosion. On the other hand, the corrosion current I_{corr} of the SAMs only was very low to the rate of reduction, less than one order of magnitude. It can see that the corrosion current of curve 2 was achieved low I_{corr} and higher E_{corr}, which indicated that the concentration of self-assembled molecules plays an important role in the corrosion resistance of the film. The AC impedance of different concentrations of self-assembly were tested in the Figure 11. As can be seen from the figure 11, the low-frequency region instability and the high-frequency curve were relatively smooth. the AC impedance value of 0.10 mol/L of SAMs could

reach 10^5 Ω • cm^2, which was two orders of magnitude higher than 0.06 mol/L and 0.18 mol/L (10^3 Ω • cm^2). The results indicated that the 0.10 mol/L of self-assembled protective aluminum alloy had more advantages than others. It can be inferred that, due to the superhydrophobic surface of the film, electrolyte ions were not easy to penetrate the film to reach the surface of the metal substrate, which maked the film play a very good barrier role. Therefore, 0.01ml/L of BTESPT was the best concentration parameter.

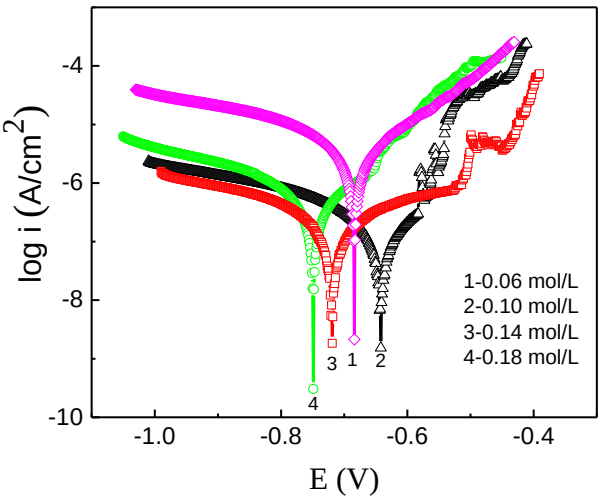

Figure 10. Potentiodynamic polarization curves of different BTESPT concentrations in 3.5 wt.% NaCl solution.

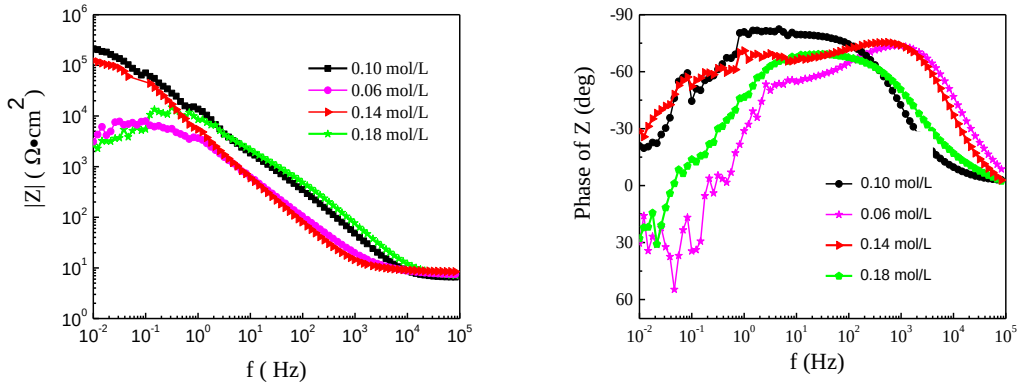

Figure 11. AC impedance plots of different BTESPT concentrations in 3.5 wt.% NaCl solution.

In order to further study the corrosion resistance of the SAMs. The corrosion resistances of the self-assembled films and the aluminum alloy specimens were investigated by the potentiodynamic polarization curves and AC impedance in 3.5 wt.% NaCl solution at room temperature (Fig. 12). I_{corr} calculated from the Tafel extrapolation of the potential polarization curve (Figure 12a). The corrosion resistance was calculated from the following Stern-Geary equation:

$$R_p = \frac{\beta_\alpha \beta_c}{2.3I(\beta_\alpha + \beta_c)}, \qquad (1)$$

βa βc represented the slope of the Tafel curve of the anode and cathode, respectively. The SAMs corrosion current density was calculated by measuring the polarization resistance at the

corrosion potential to obtain a current density of 1.140×10^{-7}A/cm^2. It is two orders of magnitude smaller than Zhu et al[38]. The corrosion current density of the BTESPT self-assembled was significantly reduced. The corrosion potential was shifted by 0.380 V than matrix. The SAMs had a $Q_{coat\text{-}T}$ of 2.632×10^{-7} F, which was much smaller than 1.3015×10^{-5} F of the bare aluminum molecules capacitance. And it can be seen that the SAMs had the highest impedance than aluminum alloy substrate at all frequencies (Figure13). These results indicate that SAMS had a better corrosion resistance trend because it had lower I_{corr} and higher E_{corr}. This may be due to the super-hydrophobic properties of SAMs surface to improve the corrosion resistance of the metal surface [39-41].

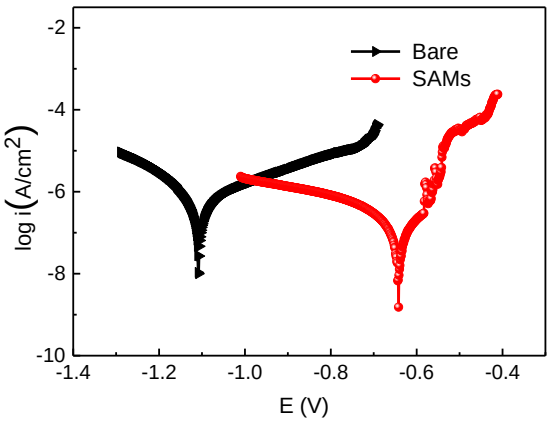

Figure 12. Potentiodynamic polarization curves of the SAMs and aluminum alloy in 3.5 wt.% NaCl solution.

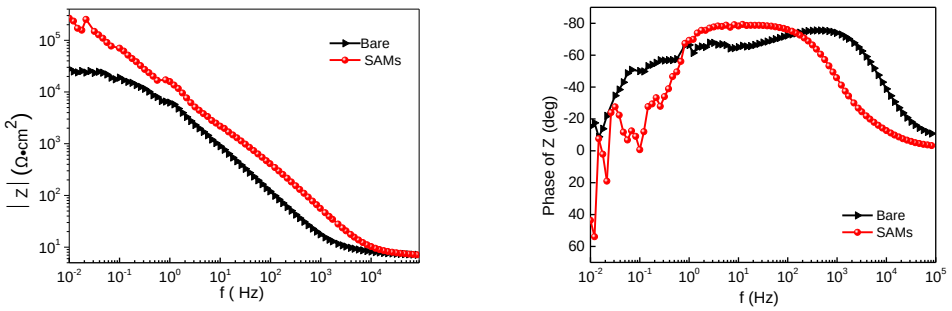

Figure 13. AC impedance plots of the SAMs and aluminum alloy in 3.5 wt.% NaCl solution.

3.3 Immersion test

For further study the corrosion resistance of SAMs and aluminum alloy substrates, they were immersed in 3.5 wt.% NaCl solution for 120 hours (Figure 14). After immersion for 24 hours, no obvious corrosion occurred on the SAMs and the aluminum alloy substrate. With the increase of time, the corrosion of aluminium alloy matrix began to appear, but the corrosion of SAM film did not occur. After 48 hours, corrosion spots were appeared on the bare aluminum surface, and the corrosion began to be serious with the increase of immersion time. The crack of the aluminum alloy substrate was emerged and accumulated corrosive material at 120 hours. On the other hand, only 120 hours later, a small crack appeared in the self-assembled monolayers after 120 hours. At the same time, the

corrosion of the aluminum alloy matrix was very serious. The SAMs had no serious damage, and it still had a good protective effect on the aluminum alloy substrate [42-46]. It can be concluded that the self-assembled film had corrosion resistance and was helpful to protect the aluminum alloy.

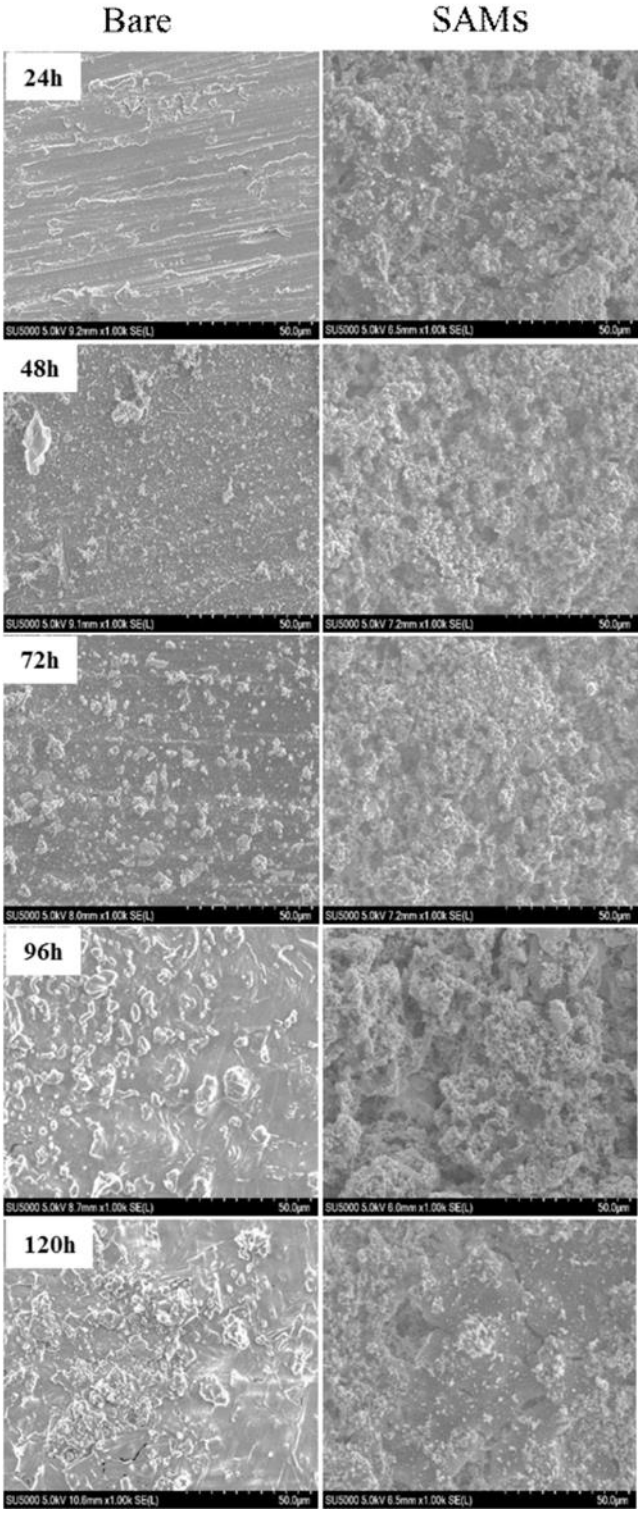

Figure 14. SEM of the SAMs and Aluminum alloy immersion in 3.5 wt.% NaCl solution.

4. CONCLUSIONS

In this paper, a superhydrophobic and corrosion-resistant self-assembled film was prepared on aluminum alloy substrates by chemical corrosion and self-assembly. The results show that the concentration of BTESPT was 0.10 mol/L. The morphology of BTESPT molecules were uniform, dense and stacked together. The contact angle of the SAMs was 158±2°, indicating good hydrophobic performance. Moreover, the results of EDS, FTIR and XPS indicated that the self-assembled films had been successfully prepared on the surface of aluminum alloy. The electrochemical properties of the films were measured by polarization curves and AC impedance in 3.5wt.% NaCl solution at room temperature. The results showed the corrosion current density of the SAMs was 1.140×10^{-7}A/cm^2, and the AC impedance was 2.30×10^5 Ω • cm^2, which indicated that the films had a certain resistance corrosion performance. The results of immersion test showed that the SAMs had better durability and stability in 3.5 wt.% NaCl solution. In conclusion, the results show that when the concentration of self-assembled films was 0.10 mol/L, the SAMs had good corrosion resistance and hydrophobic properties. The SAMs was helpful to protect the aluminum alloy.

ACKNOWLEDAGEMENT
The authors thank the financial supports from the National Natural Science Foundation of China (No. 51665010 and No. 51664011), and the Guangxi Key Laboratory of Electrochemical and Magnetochemical Functional Materials (No. EMFM20181106).

CONFLICT OF INTEREST
The authors declare no conflict of interest.

References

1. S.L.Zheng, L.Cheng. Q.Fu, M.Li, W. Hu, Q.Wang, M.Du, X. Liu and Z.Chen. *Surf. Coat. Technol* **.,** 276 (2015) 341.
2. M .Hancer, H. Arkaz, *Appl. Surf. Sci*.,354(2015**)** 342 .
3. B- Ou Wan. D. Lv. M.Xue, F .Wang and H.Wu, *Surf. Interface Anal.*, 48(2016) 173 .
4. Y.Liu, J.Liu, S.Li, Y,.Wang, Z .Han, L. Ren, *Colloids Surf., A*., 466(2015) 125.
5. SP.Rodrigues, CFA.Alves, A .Cavaleiro, S.Carvalho, *Appl. Surf. Sci*., 422(2017) 430.
6. V. Z.Pokhmurskii, I.V. Vynar, and L .Bily, *Corros. Sci*., 53 (2011)904.
7. M.Ilman, *Int. J. Fatigue.*, 62(2014) 228.
8. AS,.Nguyen, M.Musiani, ME,.Orazem, N,.Pébère, B .Tribollet, and V .Vivier, *Corros. Sci.*, 109(2016) 174.
9. J.Telegdi, G.Luciano, S .Mahanty, and T.Abohalkuma, *Mater. Corros*., 67(2016) 1027.
10. J.Lee, J.Bong, Y-G.Ha, S.Park, and S Ju, *Appl. Surf. Sci.*, 330(2015) 445.
11. W.Xiao, R.Man, C.Miao and T.Peng, *J. Rare Earths*., 28(2018) 117.
12. Q, Zhang, Y,.Hua, C.Xu, Y.Li, J.Li and P.Dong, *J. Rare Earths.*, 33(2015) 1017.
13. CA.Grillo, F .Alvarez MA.Mele. *Colloids Surf., B*., 117(2014) 312.
14. L.Qin, W.Zhao, H.Hou, Y.Jin, Z.Zeng, X .Wu and Q . Xue, *RSC Adv.*, 4(2014) 60307.
15. Y.Wu, W.Zhao, W.Wang, and W.Sui, *RSC Adv.*, 6 (2016) 5100.
16. H.Zhu, L.Yue, C.Zhuang, Y.Zhang, X.Liu, Y .Yin, and S.Chen, *Surf. Coat. Technol*., 304(2016) 76.
17. BP.Singh, BK.Jena, S. Bhattacharjee and L .Besra, *Surf. Coat. Technol.*, 232(2013) 475.

18. S.Zheng, C.Li, Q.Fu, W.Hu, T.Xiang, Q.Wang, M.Du, X .Liu, and Z.Chen, *Mater. Des*., 93(2016) 261.
19. B.Zhang, X.Zhao, Y .Li and B. Hou, *RSC Adv*., 6(2016) 35455.
20. T.McCallum, SP.Pitre, M.Morin, JC.Scaiano and L. Barriault, *Chem. Sci*., 471(2017) 177 .
21. Y.Su, Y.Li, R.Ganguly, and R.Kinjo, *Chem. Sci*., 379*(*2017) 55.
22. Y.Liu, H.Cao, Y.Chen, S. Chen, and D.Wang, *RSC Adv*., 6 (2016) 2379.
23. D.Wang, Y. Ni, Q .Huo, and D . Tallman, *Thin Solid Films*., 471(2005) 177 .
24. ZS.Saifaldeen, KR.Khedir, MT,.Camci, A.Ucar, S.Suzer, and T. Karabacak, *Appl. Surf. Sci.*, 379(2016) 55 .
25. VMS.Muthaiah, and S. Mula, *J. Alloys Compd.*, 688(2016) 571.
26. C.Wang, X .Zhang, and M .Su,. *Mater. Lett.*, 205(2017) 6.
27. A.Esmaeilirad, MV.Rukosuyev, J.MBG and V Veggel, FCJM . *Surf. Coat. Technol*., 285(2016) 227.
28. Y. Shen, J.T.Feng, W. Shi, C.C.Qiu, Int. J. Electrochem. Sci., 14 (2019) 2136.
29. A. S. Fouda1, S. A. Abd El-Maksoud, A. El-Hossiany, A. Ibrahim, *Int. J. Electrochem. Sci.*, 14 (2019) 2187.
30. S.G. Yao, Y.H. Zhao, X.F. Sun, D. P. Ding, J. Cheng, *Int. J. Electrochem. Sci.*, 14 (2019) 2160.
31. B.W. Feng, R Lin, D.C. Liu, D.Zhong. *Int. J. Electrochem. Sci*. 14 (2019) 2175.
32. Y.P. Zhang, H.Z. Zhu, C. Zhuang, S.G. Chen, L.Q. Wang, *Mater. Chem. Phys*., 179 (2016) 80.
33. S.G. Chen, Y.C. Cai, C. Zhuang, M.Y. Yu, X.W. Song, Y.P. Zhang. *Appl. Surf. Sci*., 331 (2015) 315.
34. R. Zhao, X.B. Gao, Y.L. Lu, F.Z. Du, L. Zhang, D.Z. Liu, X.F. Chen**.** *Mater. Res. Express*., 5 (2018) 046515.
35. H.Z. Zhu, L.F. Yue, C. Zhuang, Y.P. Zhang, X.L. Liu, Y.S. Yin, S.G. Chen, *Surf. Coat. Technol*., 304 (2016) 76.
36. L. Lei, J. Shi, X. Wang, D. Liu, H.G. Xu, *Surf. Coat. Technol*., 376 (2016) 161.
37. Y.Q. Wen, H.M. Meng, W. Shang, *RSC Advances*., 5(2015) 80129.
38. G.S. Hikku, K. Jeyasubramanian, A. Venugopal, Rahul Ghosh*, J. Alloys Compd.,* 716 (2017) 259.
39. C,Liu, F Su, and J .Liang, *RSC Adv*., 4(2014) 55556.
40. L.Feng, Y.Che, Y,.Liu, X .Qiang, and Y.Wang, *Appl. Surf. Sci*, 283(2013) 367.
41. H. Z. Zhu, L. F Yue, C. Zhuang, Y. P Zhang, X. L. Liu, Y. S. Yin, S. G. Chen, *Surf. Coat. Technol.*, 304 (2016) 76.
42. Y,.Ding, Y.Li, J. Lin, and C . Wen, *J. Mater. Chem. B.*, 3 (2015) 3714.
43. H Moghanni-Bavil-Olyaei, and J. Arjomandi, *RSC Adv*. 6(2016) 28055 .
44. Q.Wang, H.Miao, Y,.Xue, S.Sun, S. Li, and Z.Liu, *RSC Adv*., 7(2017) 25838.
45. X.Ren, S.Xu, S.Chen, N.Chen, and S.Zhang, *RSC Adv*., 5(2015) 101693.
46. N.Chaubey, V-S Savita, and MA.Quraishi, *J. Assoc. Arab Univ. Basic Appl. Sci.*, 22(2017) 38.